

Sunlight degradation of methylene blue and depollution of biomethanated spent wash on W/Mo-doped TiO₂

Rokhsareh Akbarzadeh, Vikram S. Ghole, Abbasali Khodadadi

Abstract— Films of 1.0 wt% tungsten- and tungsten-molybdenum-doped TiO₂ on glass substrates were prepared by a simple sol-gel dip-coating using titanium peroxide gel and employed for photocatalytic degradation of methylene blue (MB) and depollution of biomethanated spent wash (BSW) in sunlight. The doped TiO₂ samples were characterized by scanning electron microscopy (SEM), X-ray diffraction (XRD), UV-VIS spectroscopy. The influences of the dopants and annealing temperature on the size, morphology and optical properties of TiO₂-based photocatalysts were investigated. TiO₂ films heat-treated at 500°C and Mo/W-codoped TiO₂ photocatalysts showed the highest photocatalytic efficiency for degradation of biomethanated spent wash and methylene blue in sunlight, respectively.

Index Terms— W-Mo/TiO₂; biomethanated spent wash; Methylene blue; photocatalyst

I. INTRODUCTION

Anaerobically-treated (biomethanated) spent wash (a brown liquid waste as a by-product of the distillation of fermented molasses) still contains high concentrations of organic pollutants, which are refractory to biological treatment. The color of this wastewater is primarily attributed to dark brown pigment (melanoidins) as well as the presence of phenols, caramel and melanin [1-2]. The spent wash can be profitably subjected to anaerobic treatment to produce gases of fuel value [3], however, the treatment is not effective for complete decolorization and mineralization.

In recent years, heterogeneous photocatalysts such as TiO₂, ZnO, Fe₂O₃, CdS, GaP and ZnS offer high potential for elimination of ambiguous refractory organics. Among the semiconductor catalysts, titanium dioxide (TiO₂) has received the greatest interest in photocatalysis technology. The TiO₂ is the most active photocatalyst under photon energy of 300 nm λ <math>< 390\text{ nm}</math> and remains stable after repeated catalytic cycles, whereas CdS or GaP are degraded and to produce toxic products [4]. In addition, the multi-faceted functional properties of TiO₂ catalyst, such as their chemical and thermal stability or resistance to chemical breakdown and their strong mechanical properties have promoted its wide application in photocatalytic water

treatment [5]. Since the band gap energy (E_g) of TiO₂ is high, considerable efforts have been directed to extend the absorption edge of TiO₂ towards the visible part of the spectrum in the last three decades. Different solutions have been investigated and proposed by scientists such as doping titania with metallic [6-8] and non-metallic species [9-11] and loading other semiconductors [12-13] on the surface or into the crystal lattice of titania.

Titania powder is used for photocatalytic degradation of pollutants in aqueous solution using a photocatalytic reactor and it is difficult to separate them. Thin films of titania as an active photocatalyst would be an attractive alternative to overcome the catalysts separation problems. TiO₂ thin films have been receiving much attention in the past years as their chemical stability, high refractive index, and high dielectric constant allow their use as components in optoelectronic devices, sensors and photocatalysis [14].

Titanium oxide films have been made by a variety of techniques. Among the different methods for the preparation of thin TiO₂ electronic layer, sol-gel method has many advantages; particularly the possibility of producing large surfaces and the method is also suitable for deposition on different substrates [15-19]. This process is carried out at room temperature [20]. The sol-gel technique has emerged as one of the most promising techniques as this method produces samples with good homogeneity at low cost [21]. It is particularly attractive for thin films fabrication, because the liquid precursor can easily be applied on a substrate by dipping.

In this work, TiO₂, W-doped TiO₂, Mo/TiO₂ and Mo/W-codoped TiO₂ films on glass substrates were synthesized, characterized, and applied for photocatalytic degradation of methylene blue (MB) and depollution of biomethanated spent wash (BSW) in sunlight. The only published paper on solar photocatalytic degradation of anaerobically treated distillery wastewater using TiO₂ powder by Ziadi et al in 1995 [22] and we are reporting solar treatment of biomethanated spent wash using TiO₂ thin film for the first time here. Also the codoped Mo/W/TiO₂ for the first time successfully used for treatment of dyes such as methylene blue, malachite green and methyl violet in this study.

Peroxopolytungsten acid for doping of TiO₂ was obtained via dissolution of tungsten acid into hydrogen peroxide which is reported elsewhere [23] Di Paolo et al (2002) prepared W, V and molybdenum doped TiO₂ [24]. In another study later they concluded that TiO₂/W (which was prepared by using the wet impregnation method) was the most efficient sample for the photodegradation of benzoic acid [25]. The W addition causes a red shift of the optical

Manuscript received July 19, 2014.

Rokhsareh Akbarzadeh, Department of Environmental Sciences, University of Pune, Pune 411007, India

Vikram S. Ghole, Department of Environmental Sciences, Vasantdada Sugar Institute, Pune 412307, India

Abbasali Khodadadi, Department of Chemical Engineering, University of Tehran, Tehran, Iran

absorption related to a decrease of the band-gap energy, which increases the photocatalytic activity of titania after UV radiation as well as in the visible-light region with respect to undoped titania [26].

Matrilas and his colleagues found that Molybdenum species supported on anatase were less active for oxidation of toluene than vanadium and, in addition, the presence of molybdenum inhibited the interaction between vanadium and anatase leading to poor vanadium dispersion [27]. Haber et al (2008) reported that many aromatic compounds were effectively oxidized on MoO₃/TiO₂/Ti electrodes in either aqueous or non-aqueous (acetonitrile) solutions [28]. To best of our knowledge the photocatalytic activity of codoped W-Mo/TiO₂ is not reported elsewhere.

II. EXPERIMENTAL

A. Preparation of TiO₂ and its doping with molybdenum, tungsten and molybdenum-tungsten

The sol-gel solution was prepared similar to the procedure explained in our earlier work [29], briefly as follows: 4.2 gram titanium butoxide was hydrolyzed by adding 100 ml distilled water and washed out 2 times (every time with 50 ml) and thus produced water-alcohol solution was removed by simply decantation of water from the formed white precipitate. To this formed white precipitate 15 ml of 30% hydrogen peroxide solution was added to produce the sol of titanium oxide; simultaneously 65 ml of water was added to this solution with continuous stirring to maintain the temperature of reaction and dilute the solution. When this solution got visibly viscous, the glass rings and slides were dipped into the solution and pulled up for single coating before gelling (gelling of solution at room temperature take place between 30-60 minutes). A known amount of the glass rings and slides also left in the solution till it get dry in the room temperature during 3-4 days (which gives the multilayer of coating). Process variables such as solution concentration (Ti (OC₄H₈)₄: H₂O₂: H₂O), gelling time (30min) and annealing time (3hours) remained constant. The dip coated glass rings for photocatalytic test and slides for characterization were left to dry at ambient temperature for several days followed by heating up to 100°, 300°, 500° and 600°C in a furnace at an ascending heating rate of 2°C/min (start point was 2°C/min when reach to 100°C then the temperature rate increased to 5°C/min, after 30 minutes it increased to 10°C/min and finally 20°C/min till it reached to 500 °C). Weights of the films formed on the glass rings were measured by the difference in weights gained by coating on known quantity of glass rings after heating. The film thickness on the rings estimated about 790nm.

14 mg of Molybdenum trioxide powder and/or 15 mg of tungstic acid (both from Merk) were separately dissolved in 2 ml of 30% H₂O₂ solution and water at 100°C to obtain molybdenum peroxide and peroxopolytungstic acid solutions, respectively. The solutions were added to the titanium peroxy sol (above mentioned titanium peroxide solution) while stirring to prepare 1.0wt% tungsten, molybdenum and tungsten-molybdenum-doped titanium oxide separately. For co-doping of titanium peroxy solution,

both molybdenum peroxide and peroxopoly tungsten were added together to the peroxy solution while stirring.

B. Characterization

The surface morphology and elemental analysis of the samples were obtained by using SEM (JSM 6360A, JEOL) operated at 20kV. The crystal structures of dried TiO₂ powder and films were investigated by X-ray diffraction (Bruker AXS D8) (XRD). The dried powder and the films on glass slides that were gradually heated up to 500°C were characterized by XRD. Almost all the information about the crystal structure of the films comes from the lattice planes parallel to the substrate surface. For a film coated on glass, the X-ray diffraction pattern was obtained by grazing incidence angle (GIA) technique. The fixed grazing incidence geometry has the advantage of substantially limiting the substrate diffraction peak intensity, since the X-rays penetrate less into the layers [30]. The absorbance spectra of the powder and films were recorded by using UV-vis spectrophotometer (JASCO model V-670).

C. Photocatalytic activity test

Aqueous MB (10⁻⁷ and 10⁻⁴ M) solution was prepared and used to evaluate the photocatalytic activity and kinetic study of thin films. MB is used by most of the researches to test the activity of catalysts; therefore MB was chosen as a model pollutant for easier comparison of the results with previous works which are carried out in this area. For photocatalytic degradation of MB, the heat treated and coated glass rings with TiO₂ or/& doped TiO₂ films were used as photocatalyst.

To a small glass bottle containing coated glass rings (3g of coated rings which contain 0.001g thin film) 10 ml of MB (10mg/l) solution was added and then was kept in the sunlight. UV-VIS spectra of sample were recorded at different time intervals by UV-Vis spectrophotometer and the MB concentration was estimated using these results.

For photocatalytic degradation of BSW, the same procedure as for MB was followed. The photocatalyst, coated glass rings (3g glass rings=0.001g catalyst), were taken into a glass bottle containing 10 ml of diluted BSW with initial COD of 22800 mg/l and dark brown in color (10, 50, 100, 300 and 500 time dilution) and then glass bottles were exposed to the sunlight.

The changes in the color of irradiated BSW samples during photo-degradation were monitored using UV-VIS spectrophotometer against time and previous to this, reduction of COD along with reduction in UV-Vis absorbance was examined. To determine the rate of degradation of BSW without photocatalyst, a control experiment was carried out by adding same quantity of uncoated glass rings to a glass bottle containing 10 ml of BSW and irradiating under identical condition. The performance of photocatalytic reaction for treatment of BSW against time was also determined by COD test, the method described in Standard Methods (APHA 4th ed.1995) [31].

III. RESULTS AND DISCUSSION

A. Characterization of TiO₂ and W- and Mo-W-doped TiO₂

The titanium oxide powder before heat treatment is amorphous in structure. Thermal treatment up to 500 and 600 °C for 3 hrs, results in well crystallized anatase-type TiO₂.

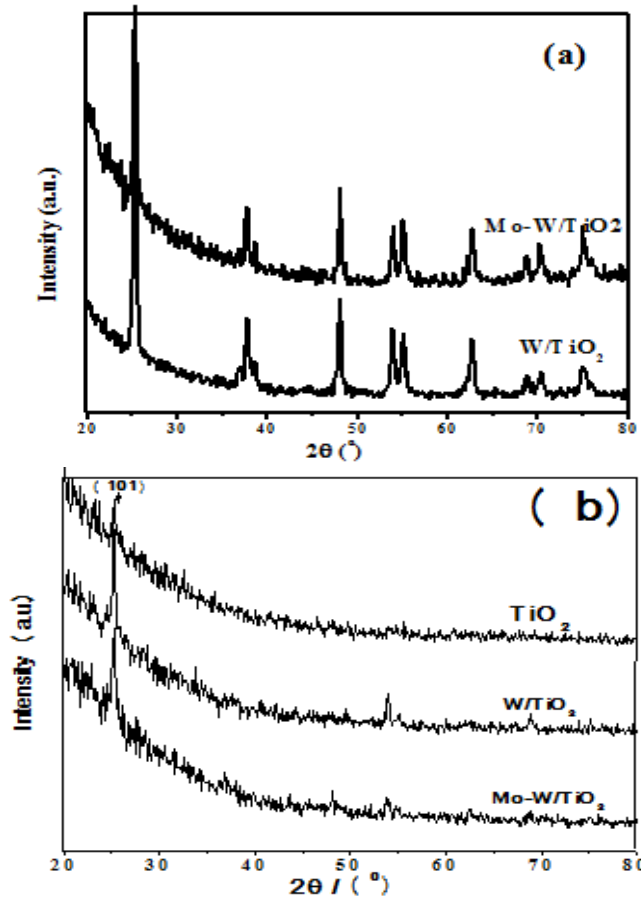


Fig. 1. XRD patterns of TiO₂, W- and Mo-W- doped powders (a) and films (b)

Fig. 1a shows the XRD patterns of the samples of W- and Mo/W-doped TiO₂ in the form of powder (pure and Mo are not shown but available in different format), All samples show the anatase phase except Mo/TiO₂ which shows forming of rutile phase too. Fig. 1b depicts the X-ray diffraction pattern of the sol-gel derived films coated on glass after heat treatment up to 500°C. Also, after doping, it is found that the major diffraction peaks are attributed to the anatase TiO₂ phase and no other peaks related to dopants or impurities are observed that may incorporate in titanium dioxide anatase phase. Bragg reflections at angles of 25.3°, 48.1° and 55.6° in doped film corresponded to (101), (200) and (211) tetragonal crystal planes of anatase phase of TiO₂, respectively. The anatase phase is the most active one for photocatalytic reactions [32].

From the full-width-at-half-maximum (FWHM) of the strongest peak (101) anatase phase, crystallite sizes were calculated using Scherrer's equation as follow:

$$T = k\lambda / (\beta \cdot \cos\theta) \quad (1)$$

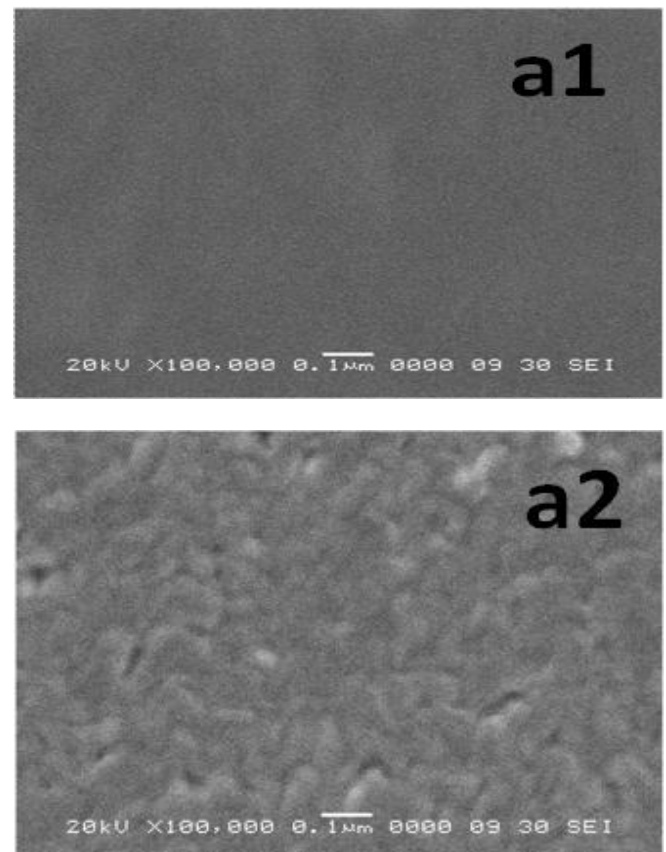
Where T is crystallite size and K, λ, β and θ are constant, wavelength, FWHM and angle, respectively. The

calculated crystallite sizes of pure and W-and/or Mo- doped TiO₂ in the form of powder and film is shown in Table 1. However there was not a clear relation between doping and particles size.

Photocatalyst		TiO ₂	W/TiO ₂	Mo-W/TiO ₂
Powder	crystallite size (nm)	12.3	21.4	27
Film	crystallite size (nm)	35	19.8	20.3
Band gap (eV)		2.88	2.81	2.31

Table1: Crystallite sizes and band gap of TiO₂ and Mo and/or W-doped TiO₂ samples calcined at 500°C

A Pt thin film was sputtered on the photocatalysts films and examined by scanning electron microscopy (SEM) to investigate their surface morphology (Fig. 2). The single-coat samples of TiO₂ and W/TiO₂ show no distinguished particles and are transparent and homogeneous without any cracks over a wide area (Fig.2 a-1 and b-1). However, the multicoated samples of TiO₂ and W- and Mo-W- doped ones show rod-like nanoparticles of about 30 nm diameters and 100 nm lengths. The multicoated films are highly porous and allow diffusion of pollutants onto the photocatalyst surface with no limitation. The film thickness estimated from the weight gain of the glass substrate is about 790 nm for multicoated films. The films extended over the glass substrates enhance the easy access of pollutants to the photocatalyst surface and photo-efficiency. The adhesion and activity of multicoated films are enough for all cycles.



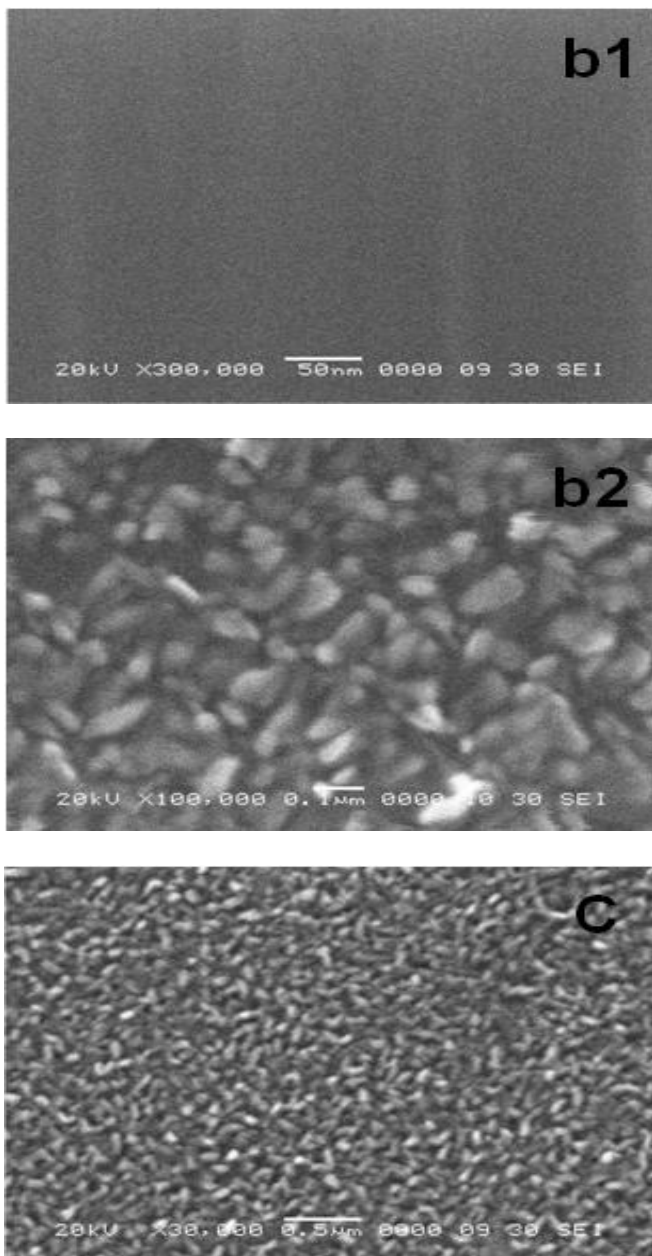


Fig. 2 SEM micrographs of films on glass calcined at 500°C, a-1) single and a-2) multi-coat TiO₂ b-1) single and b-2) multi-coat W/TiO₂ c) multi-coat film of Mo-W/TiO₂.

B. UV-Vis spectroscopy

Fig 3 shows the absorption spectra of the samples in the form of powder. It shows the UV-Vis spectra of Degussa TiO₂ and synthesized TiO₂, W- and Mo-W-doped TiO₂ powder samples, the cutoff wave lengths of which are 400, 430, 440 and 536 nm, respectively. The results show a significant absorption edge red-shift of TiO₂ powder and the one doped with tungsten, as compared to Degussa TiO₂ sample. A further considerable red-shift of about 100 nm is observed for the Mo/W-doped TiO₂ sample. An additional absorption peak shoulder from about 430 to 700 nm is observed for TiO₂ powder and the one doped with tungsten. The Mo/W-doped sample shows two absorption peaks in the range of about 536-850 and 850-1200 nm. Band gap estimation of samples was performed on the basis of equation (1) and the results are presented in Table 1, using Fig. 5 UV-Vis spectra.
 $E = hc/\lambda$ (1)

Where, E is band gap energy, h is Planks constant (6.626×10^{-34} Joules.sec), C is the speed of light (3×10^8 m/s) and λ is cut off wavelength.

The band gap of Degussa TiO₂ is estimated to be 3.09 eV, while those of the prepared TiO₂ and the ones doped with tungsten and molybdenum-tungsten are significantly lower. 0.78 eV narrowing of the band gap is observed for Mo/W-doped TiO₂ sample, due probably to synergetic effect of W and Mo doping.

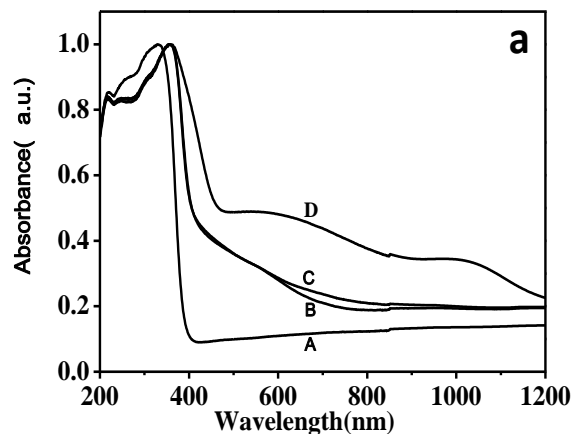
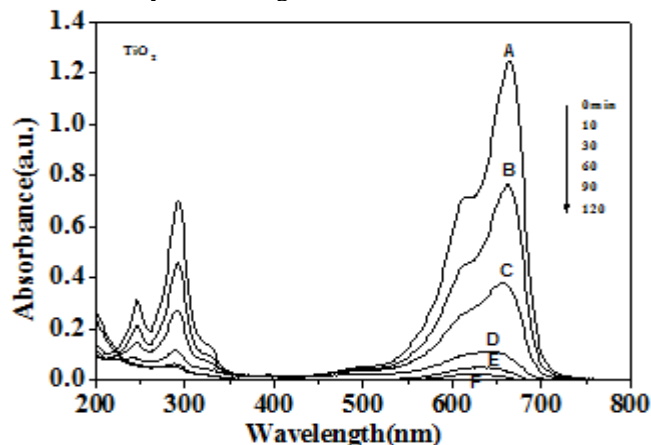


Fig. 3 Normalized UV-Vis spectra of A) TiO₂ Degussa, B) TiO₂, C) W-TiO₂ and D) Mo/W-TiO₂ powder heat treated at 500°C

C. Photocatalytic treatments of MB and kinetic

Photocatalytic activity of films deposited on glass rings was tested for degradation of MB (8-32 mg/L solution) under UV and solar radiation. A cationic form of MB can be reduced and changed from blue to colorless by accepting a photo-catalytically generated electron [33]. The rate of discoloration of MB decreased with increasing initial concentration of MB when other parameters were kept unchanged. Therefore, the photocatalytic discoloration of MB was found to be pseudo-first order reaction and its kinetics may also be expressed as;
 $\ln(A/A_0) = kt$

Here k is the apparent rate constant, A₀ is the initial absorption of methylene blue, t is the reaction time and A is the absorption of aqueous MB at time t. The rate constant, k is determined by a linear regression method.



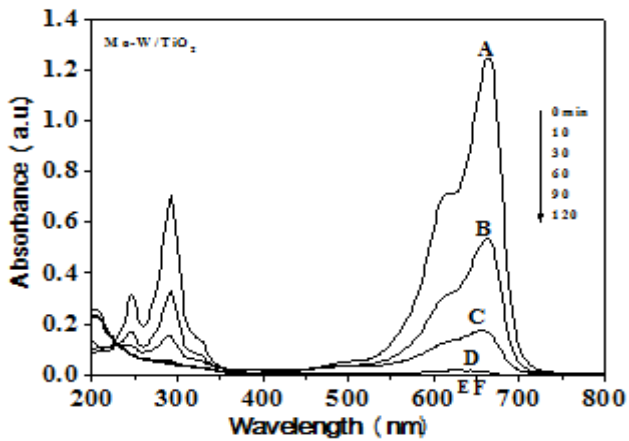


Fig. 4 Degradation of MB in sunlight, using a) TiO₂ and b) Mo/W-TiO₂ films heated at 500°C in air.

UV-Vis spectra of the MB in the presence of TiO₂ and Mo/W-doped TiO₂ films before and after solar light irradiation at different time intervals are presented in Fig. 4. The same experiment was carried out for the control sample at identical conditions. There is a sharp reduction in intensity of the peak at 664 nm during first 30 minutes of sunlight irradiation in the presences of photocatalyst.

664nm peak intensity of MB shows that about 100 % degradation of MB took place after 2 h exposure to sunlight in the presence of pure TiO₂ films. This time reduced to 1 h in the presences of Mo/W-doped photocatalyst. In the first 10 minutes the rate of MB removal in the presence of Mo/W-TiO₂ films was 52 % while it was 36% for pure TiO₂ films, showing photocatalytic activity enhancement due to co-doping. The plot of the percentage MB degradation in the absence of TiO₂ film for the same time of irradiation was done for comparison and it suggests that degradation of MB was quite slow without photocatalyst which occurs due to photolysis only. Based on the results of MB degradation, the first order kinetic plots were prepared. The plot of $\ln(A/A_0)$ against time of irradiation for TiO₂ and doped TiO₂ is shown in Figs. 5. All the lines of kinetic plots are linear, which confirms the first-order reaction kinetics. These kinetic plots have been utilized for calculation of rate constant values for each degradation reaction. Result of the catalytic activity test shows the highest rate for degradation of MB in sunlight as well as UV light refers to Codoped W-Mo/TiO₂. This degradation rate increased in the sunlight.

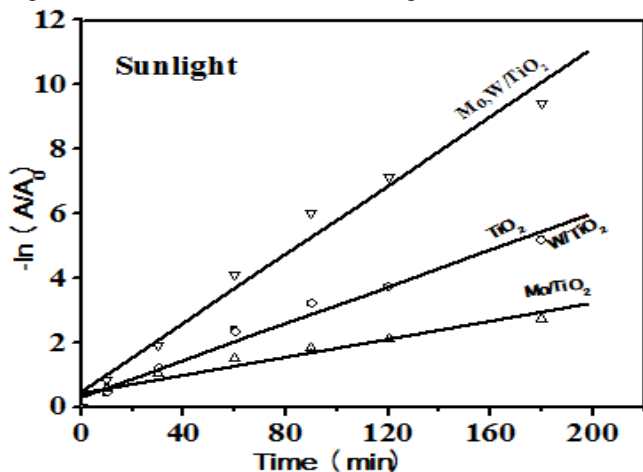


Fig. 5 kinetics of MB degradation in the presence of pure and doped titania film in sunlight

The absorption reduction in the case of using films heat treated at different temperatures was recorded. Rate constant of TiO₂ calcined at 500°C was 1.3, 1.5 and 3.9 time faster than TiO₂ calcined at 600, 300 and 100°C respectively (Table 2).

Films treatment at (°C)	heat	Rate constant (min ⁻¹) in sunlight	R ²
100		0.01097	0.87243
300		0.02875	0.99806
500		0.04258	0.99915
600		0.0335	0.97759

Table2: Reaction rate constants for the removal of methylene blue under sunlight using films prepared at 4 different temperatures

As comparison in the doped photocatalysts, the highest activity for degradation of MB was observed for co-doped Mo/W-TiO₂ heat treated at 500°C. It shows the activity of TiO₂ after doping with W and Mo, W goes up comparing with pure TiO₂ but doping of TiO₂ with the Mo reduces the activity of photocatalyst. The results are summarized in Table 3.

Photocatalyst	TiO ₂	Mo-TiO ₂	W-TiO ₂	Mo/W-TiO ₂
% MB degradation after 1 h	91.2	78.4	93.6	99.2
Time for complete degradation (h)	2	4	1.8	1.2
Rate constant (min ⁻¹)	2.871*10 ⁻²	1.401*10 ⁻²	2.860*10 ⁻²	5.340*10 ⁻²

Table3: Kinetics of photocatalysts for degradation of methylene blue (MB) in sunlight

D. Catalysts recycle for discoloration of MB

In order to find out the life span of the film and to check the recyclability of the photocatalyst after MB degradation, the procedure followed was: the colorless solution was decanted and fresh MB solution was added to the beaker containing film catalyst and was kept in the sunlight for decomposition of the fresh MB solution. After repeating this for 20 cycles the photocatalyst had almost the same capacity to degrade MB. The adsorbed MB on the film surface also did not remain for long time and it was degraded and films could be used for further cycles. Therefore in consecutive experiments, no appreciable decrease in catalytic activity was observed. The results of the 10 time photocatalyst recycle are shown in Fig. 6.

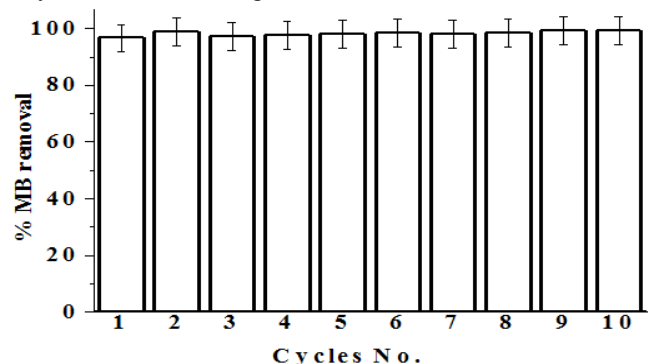


Fig. 6 Activity of catalyst in number of cycles is shown by %MB removal in each cycle.

E. Photocatalytic treatments of BSW

Photocatalytic activity of films deposited on glass rings was also tested for degradation of BSW with different dilution factors (50, 100, 300, 500 times) under solar irradiation as well as UV irradiation. The reduction in absorption in UV-Vis spectra of BSW were recorded by UV-Vis spectrophotometry, this degradation was confirmed by COD analysis. Control sample of BSW also was carried out in the identical condition in the absence of films; the reduction in absorption of BSW was negligible in this case (Fig. 7). Wavelength at 267.3 was chosen as a fix point and then absorption was plotted against time using these records at this point (fig. 8a). The plot of $\ln(A/A_0)$ with time of irradiation for BSW sample is shown in Fig. 8b, the line of kinetic plots are linear, which confirms the first-order reaction kinetic in BSW degradation.

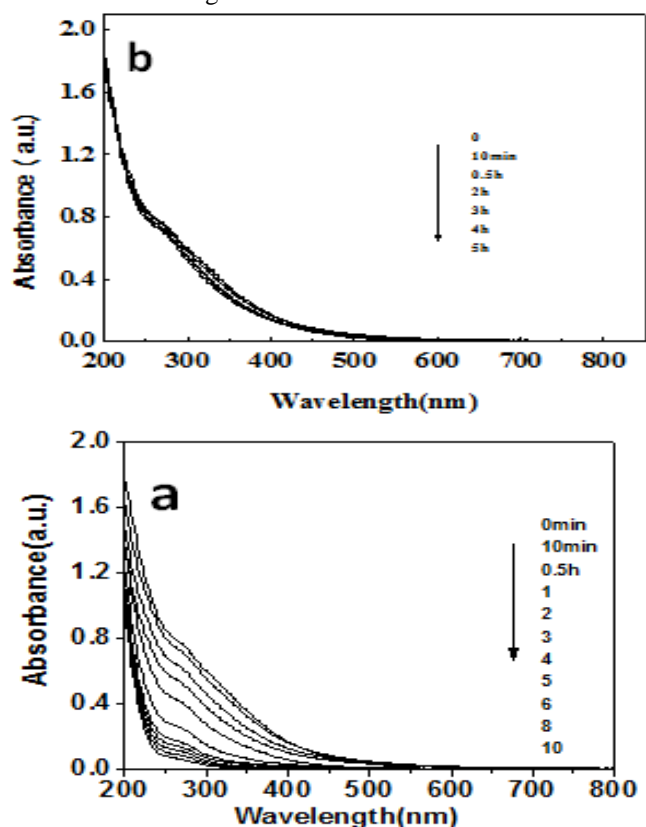


Fig. 7 Reduction in absorption of BSW against sunlight irradiation time using film heated at 500°C a) in presence of photocatalyst and b) without photocatalyst

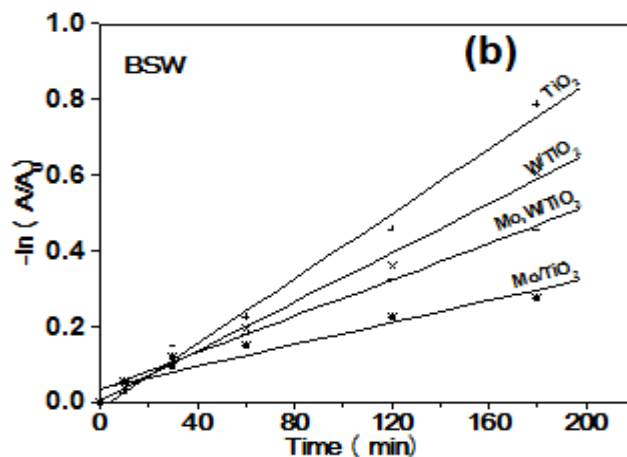
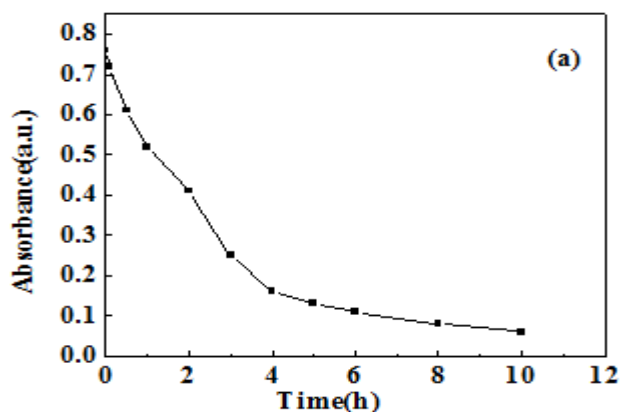


Fig. 8 Absorption (left) and kinetics (right) of BSW depollution in the presence of pure and doped titania film in sunlight

The degradation rate of BSW was measured by reduction in COD of samples. The evolution of pH also recorded along with irradiation time. It shows a reduction in pH along with reduction in UV absorbance and COD (Fig.9). To compare the activity of pure photocatalyst with doped one for treatment of spent wash it was obtained that the best result for BSW degradation, color and COD reduction was for undoped TiO₂ films heat treated at 500°C (Fig. 8b). The first order kinetics rate for TiO₂, Mo, W and Mo/W doped TiO₂ is shown in figure 8b.

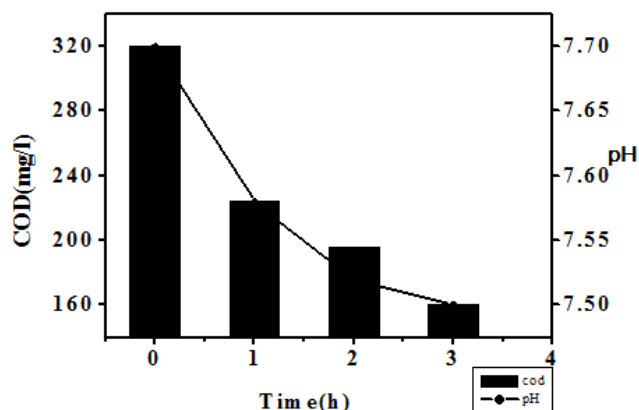


Fig. 9. COD reduction along with reduction in pH in the presence of catalyst at ambient condition

The time of color reduction as well as COD reduction increased with increasing concentration of sample. It is probably because of inhibition of color and darkness of BSW which prevent the light to penetrate the solution and reach to the active surface of photocatalyst to degrade the organics. However the rate of degradation at the beginning is high and as the concentration of pollutant comes down the kinetic rate also reduces.

The result shows that lowering the pH to neutral level before subjecting of BSW to catalysts has no significant effect on performance of this catalyst. However the photocatalytic treatment by TiO₂ thin film itself is reducing pH down to the neutral level as the degradation of organic compounds happen.

F. Catalysts recycle test for degradation of BSW

In order to find out the life span of the film photocatalyst and to check its recyclability for BSW treatment, the procedure followed was: the partly treated BSW after each 3hr was decanted and untreated BSW was added to the beaker containing film catalyst and was kept in the sunlight for decomposition of the BSW. After repeating this for 13 cycles the photocatalyst had almost the same capacity to degrade BSW. Therefore in consecutive experiments, no appreciable decrease in catalytic activity was observed.

IV. CONCLUSION

A long life, transparent, optically homogeneous TiO₂-based films undoped and doped with W- Mo- and Mo/W were prepared by simple sol-gel dip coating method using titanium peroxide gel. The films consisted of anatase TiO₂ phase after heating at different temperatures and doping with W and both of Mo, W.

The band gap energy of the TiO₂ thin films was calculated to be about 2.91 eV heated at 500°C, indicating band gap narrowing. Titanium based films photocatalyst has been found to be active for photocatalytic degradation of methylene blue as well as biomethanated spent wash in sunlight. Among TiO₂ based thin films, TiO₂ films treated at 500°C and codoped Mo/W/TiO₂ were found to be the most active photocatalyst for degradation of methylene blue. This result could be correlated to the red shift in optical absorption. Also, The TiO₂ film catalyst was found to be quite active for degradation of biomethanated spent wash, compared with other photocatalysts in sunlight.

REFERENCES

[1] M.A. Godshall, Proceeding of 6th International Symposium organized by association Andrew van Hook (AvH), March 25, 1999, Reims, France, pp.28.
[2] D.F. Kalavathi, L.Uma, Subramaniam, G., Enzyme Microb. Technol.29 (2001) 246.
[3] A. D. Pathwardhan, Industrial wastewater treatment, PHI Learning Pvt. Ltd., New Delhi, 2008.
[4] S. Malato, P. Fernandez-Ibanez, M. I. Maldonado, J. Blanco, W. Gernjak, Catal. Today. 147 (2009) 1.
[5] M. N. Chong, B. Jin, C.W.K. Chow, C. Saint, Water Research 44 (2010) 2997.
[6] B. Gao, T. M. Lim, D.P. Subagio, T. T. Lim, Appl. Catal. A: General 375 (2010) 107.
[7] Kozlova, E.A., Korobkina, T.P., Vorontsov, A. V., Parmon, V.N., Appl. Catal. A: General 367 (2009) 130.
[8] X. Chen, S. S. Mao, Chem. Rev. 107 (2007) 2891.
[9] T. Ohno, N. Murakami, T. Tsubota, H. Nishimura, Appl. Catal. A: General 349 (2008) 70.
[10] S. Higashimoto, W. Tanihata, Y. Nakagawa, M. Azuma, H. Ohue, Y. Sakata, Appl.Catal. A: General 340 (2008) 98.
[11] M. M. Joshi, N. K. Labhsetwar, P. A. Mangrulkar, S. N. Tijare, S. P. Kamble, S. S. Rayalu, Appl. Catal. A: General 357(2009) 26.
[12] M. R. Bayati, F. Golestani-Fard, A. Z. Moshfegh, App. Catal. A: General 382 (2010) 322.
[13] S. Albonetti, S. Blasioli, R. Bonelli, J. E. Mengou, S. Scire, F. Trifiro, Appl. Catal. A: General 341 (2008) 18.
[14] M. A. Hamid, I. Ab. Rahman, Malaysian Journal of Chemistry 5 (2003) 86.
[15] C. J. Brinker, G. W. Scherer, Sol-Gel Science: The Physics and Chemistry of Sol-Gel processing p21-42, Academic Press, New York, 1990.
[16] O. Harizanov, A. Harizanova, Solar Energy Materials & Solar Cells, 63 (2000) 185.

[17] J. M. Bell, J. Barczynska, L. A. Evans, K. A. MacDonald, J. Wang, D.C. Green, G. B. Smith, 13th Conference on Optical Materials. The International Society for Optical Engineering, 2255 (1994) 324.
[18] Wang Z. Hu X., Fabrication and electrochromic properties of spin-coated TiO₂ thin films from peroxo-polytitanic acid, TSE, 352(1-2), 62 (1999).
[19] C.G. Granqvist, Handbook of Inorganic Electrochromic Materials, Elsevier. 1995.
[20] R.C. Suci, E. Indera, T.D. Silipas, S. Dreve, M.C. Rosu, V. Popescu, G. Popescu, H.I. Nascu, 2009. J. Phys.: Conf. Ser 182(1), 012080.
[21] A. M Gaur, R. Joshi, M. Kumar, Proceedings of the World Congress on Engineering 2011, ISSN: 2078-0966.
[22] A.H. Zaidi, D.Y. Goswami, A.C. Wilkie, 1995. Solar 95, Processing of the American Solar Energy Society Annual Conference, 51-56, Minneapolis, MN.
[23] B. Pecquenard, H. Lecauchaux, S. Castro-Garcia, J. Livage. 13(1998) 923.
[24] A. D. Paola, G. Marci, L. Palmisano, M. Schiavello, K. Uosaki, S. Ikeda, B. Ohtani, J. Phys. Chem. B 10 (2002) 637.
[25] A.D. Paola, E. Garc-López, G. Marc, C.Martin, L. Palmisano, V. Rives, A. M. Venezia, Applied Catalysis B: Environmental 48 (2004) 223.
[26] V. Stengl, J. Velicka, M. Marikova, T. M. Grygar, ACS Appl. Mater. Interfaces 3 (2011) 4014.
[27] H. K. Matralis, Ch. Papadopoulou, Ch. Kordulis, A. Aguilar Elguezal, V. Cortes Corberan, Applied Catalysis A: General126 (1995) 365.
[28] J. Haber, P. Nowak, P. Zurek, Catal. Lett. 126 (2008) 43.
[29] R. Akbarzadeh, V. S. Ghole, Titanium Oxide Film Dried at Ambient Temperature for Photocatalytic Degradation of Methylene Blue in Sunlight. Int. J. Res. Chem. Environ. Vol.4 Issue 2 April 2014(93-99).
[30] A. R. Phani, M. Passacantando, S. Santucci, Journal of Physycs and chemistry of Solids, 63 (2002) 383.
[31] APHA (American public Health Association), Standard Method for Examination of Water and Wastewater 5220, 5-12. 1992.
[32] J. Kumar, A. Bansal, 2 (2010) 1547.
[33] Wu, J. C.-S. Chen, C.-H. J. Photochem. Photobiol. A 163 (2004) 509.